Inorg. Chem. **2008**, *47*, 9002−9009

Influence of the Metal Orbital Occupancy and Principal Quantum Number on Organoazide (RN_3) Conversion to Transition-Metal Imide Complexes

Amy N. Walstrom, Benjamin C. Fullmer, Hongjun Fan, Maren Pink, Drew T. Buschhorn, and Kenneth G. Caulton*

Department of Chemistry, Indiana University, Bloomington, Indiana 47405

Received June 5, 2008

The reaction of phenyl azide with (PNP)Ni, where PNP = $(^tBu_2PCH_2SiMe_2)_2N^-$, promptly evolves N_2 and forms a P═N bond in the product (PNP═NPh)Ni^I. A similar reaction with (PNP)FeCl proceeds to form a P═N bond but without N_2 evolution, to furnish (PNP═N—N═NPh)FeCl. An analogous reaction with (PNP)RuCl occurs with a more dramatic redox change at the metal (and N_2 evolution), to give the salt composed of $(PNP)Ru(NPh)^+$ and $(PNP)RuCl_3^-$, together with equimolar (PNP)Ru(NPh). The contrast among these results is used to deduce what conditions favor N_2 loss and oxidative incorporation of the NPh fragment from PhN_3 into a metal complex.

Introduction

Phenyl azides, and organoazides[1] in general, are frequently used to form metal imide complexes (eq 1), in a two-electron oxidation of the metal.[2−10] This can be thought of as an inner-sphere electron-transfer reaction, hence requiring an intermediate adduct $L_nM(N_3R)$, and when the metal lacks reducing power (e.g., Al^{3+}, Ag^+, and Cu^+), adducts have indeed been identified and are persistent.[11]

$$L_nM + RN_3 \rightarrow L_nM(NR) + N_2 \qquad (1)$$

Certain later-transition-metal imides (>8 d electrons) behave as if the imide ligand is electrophilic: they are attacked by nucleophiles, especially by a coordinated phosphine (eq 2).[12] Thus,[13] the reaction of PhN_3 with (PNP)Co evolves N_2, but the locus of oxidation by the resulting NPh fragment is at phosphorus, giving $[^tBu_2PCH_2SiMe_2NSiMe_2CH_2{}^tBu_2P═NPh]Co^I$, with a coordinated phosphinimine arm.

$$L_nM(PR_3) + R'N_3 \rightarrow L_nM \leftarrow N(R')═PR_3 + N_2 \qquad (2)$$

It is attractive to speculate that this cannot involve coordinated phosphorus but that instead a preliminary dissociation of the P → M bond is needed, to liberate a lone pair on phosphorus. We report here results that bear on such a hypothesis, by studying the metal dependence on the oxidation of P^{III} to P^V by imino ligands. This type of reaction is important to understand fully because it represents ligand "modification", under the oxidizing conditions available (RN_3) and thus diverts use of the M(NR) functionality from its intent,[1,14] which is normally NR transfer to olefins and cumulenes. The study of the effect of both vertical and horizontal periodic trends helps to define the influence of available d orbitals and metal−phosphine bond lability on this reaction. The comparisons offered here include Fe^{II}, Co^I, Ni^{II}, and Ni^I, hence d^6, d^8, and d^9, and then the isoelectronic comparison of divalent iron and ruthenium, all of which show distinctly different behavior toward phenyl azide. For

* To whom correspondence should be addressed. E-mail: caulton@indiana.edu.

(1) Brase, S.; Gil, C.; Knepper, K.; Zimmermann, V. *Angew. Chem., Int. Ed.* **2005**, *44*, 5188.
(2) MacBeth, C. E.; Thomas, J. C.; Betley, T. A.; Peters, J. C. *Inorg. Chem.* **2004**, *43*, 4645.
(3) Puiu, S. C.; Warren, T. H. *Organometallics* **2003**, *22*, 3974.
(4) Kogut, E.; Wiencko, H. L.; Zhang, L.; Cordeau, D. E.; Warren, T. H. *J. Am. Chem. Soc.* **2005**, *127*, 11248.
(5) Eckert, N. A.; Vaddadi, S.; Stoian, S.; Lachicotte, R. J.; Cundari, T. R.; Holland, P. L. *Angew. Chem., Int. Ed.* **2006**, *45*, 6868.
(6) Sydora, O. L.; Kuiper, D. S.; Wolczanski, P. T.; Lobkovsky, E. B.; Dinescu, A.; Cundari, T. R. *Inorg. Chem.* **2006**, *45*, 2008.
(7) Badiei, Y. M.; Krishnaswamy, A.; Melzer, M. M.; Warren, T. H. *J. Am. Chem. Soc.* **2006**, *128*, 15056.
(8) Dai, X.; Kapoor, P.; Warren, T. H. *J. Am. Chem. Soc.* **2004**, *126*, 4798.
(9) Fickes, M. G.; Davis, W. M.; Cummins, C. C. *J. Am. Chem. Soc.* **1995**, *117*, 6384.
(10) Proulx, G.; Bergman, R. G. *Organometallics* **1996**, *15*, 684.
(11) Dias, H. V. R.; Polach, S. A.; Goh, S.-K.; Archibong, E. F.; Marynick, D. S. *Inorg. Chem.* **2000**, *39*, 3894.
(12) Shah, S.; Protasiewicz, J. D. *Coord. Chem. Rev.* **2000**, *210*, 181.
(13) Ingleson, M. J.; Pink, M.; Fan, H.; Caulton, K. G. *J. Am. Chem. Soc.* **2008**, *130*, 4262.
(14) Amisial, L. D.; Dai, X.; Kinney, R. A.; Krishnaswamy, A.; Warren, T. H. *Inorg. Chem.* **2004**, *43*, 6537.

10.1021/ic801035z CCC: $40.75
Published on Web 08/30/2008

comparison, we have found that there is no reaction between d^7 (PNP)Co(O_3SCF_3) and equimolar PhN_3 under comparable conditions.

Results

Ni^I and Ni^{II}. The three-coordinate spin-triplet T-shaped molecule (PNP)Co has been shown[13] to form a coordinated phosphinimine, **2** (eq 3).

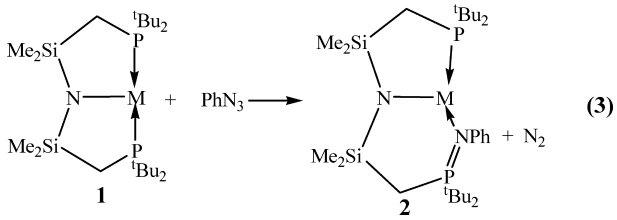

(3)

The reaction is complete at −20 °C. We now find that the same transformation occurs when M = Ni,[15] an unusual example of monovalent nickel.[16,17] There is no detectable ^{31}P NMR signal in [PNP(=NPh)]Ni, typical for a paramagnetic compound. The ^1H NMR spectrum at 25 °C, however, shows four resolved paramagnetically shifted signals due to PNP in a molecule of lower than C_{2v} symmetry; at −30 °C, each shows shifts due to the Curie−Weiss effect (i.e., shifted further away from the 0−10 ppm region at lower temperature) and now five signals are resolved; we propose that no resonances of the phenyl ring are detected because of a combination of rapid relaxation and their low intensity. Species (PNP)Ni(NPh) would be expected to be C_{2v} symmetric, so the observed spectra indicate a lower-symmetry product. The electrospray ionization mass spectrometry (ESI-MS) spectrum agrees with the formula [PNP(=NPh)]Ni.

(PNP=NPh)M crystallizes in different space groups for M = Co and Ni (Figure 1), but their molecular structures show no significant differences in the bond lengths and angles involving M. The largest difference is a 0.02 Å lengthening of M−NSi_2 from Co to Ni, and angles around M sum to 359.98° (Co) and 359.11° (Ni). The three substituents are coplanar (within 1°) at the imine N2. A best least-squares fit of the two molecules[18] shows only minor differences between Co and Ni, originating in the conformations of the M−N−P−C−Si−N1 ring, which leads to different P2−M−N1−Si1 dihedral angles: 174.8° (Co) and 148.8° (Ni).

The Ni^I center in (PNP)Ni is expected to be a potent reducing agent[15] not only because there is a relatively low oxidation state but also because it is a neutral molecule (vs a cation) and because π donation occurs from the PNP amide nitrogen. Nevertheless, the overall reaction is oxidation at P, not Ni. We suggest that reducing power is essential to this reaction because equimolar (PNP)NiCl and added PhN_3 can be recovered unchanged after 24 h at 25 °C in benzene.

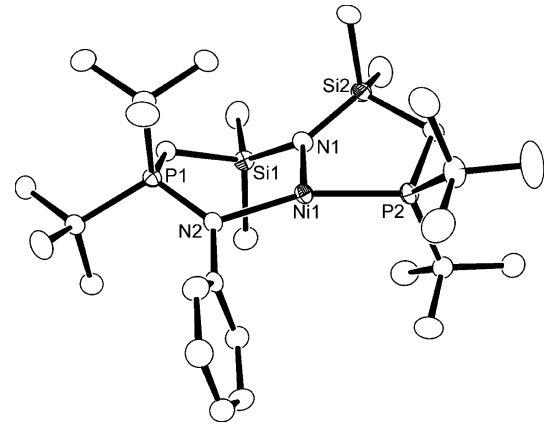

Figure 1. ORTEP drawing (50% probability) of the non-hydrogen atoms of [$^tBu_2PCH_2SiMe_2NSiMe_2CH_2P^tBu_2$NPh]Ni, showing selected atom labeling. Unlabeled atoms are carbon. Selected structural parameters: Ni1−N2, 1.9866(14) Å; Ni1−N1, 1.9929(15) Å; Ni1−P2, 2.1815(5) Å; P1−N2, 1.6153(15) Å; N2−Ni1−N1, 107.32(6)°; N2−Ni1−P2, 157.73(4)°; N1−Ni1−P2, 94.06(5)°.

No new species is detected in this mixture, so there is no simple adduct (PNP)NiCl(PhN_3) formed. The robustness of the P → Ni^{II} bonds and the absence of simple adduct formation here inhibit any loss of N_2 to create a PhN ligand. The rapid reaction with (PNP)Ni^I thus supports the idea that this electron-rich species has some σ^*_{PNi} character, which makes the P → Ni bond labile.

Fe^{II}. A comparison to (PNP)FeCl is enlightening. This molecule is a nonplanar d^6 species with a quintet ground state.[15] The reaction of (PNP)FeCl[15] with equimolar PhN_3 in toluene at −78 °C gives, upon warming toward room temperature, a color change from light brown to deep maroon, and the ^1H NMR spectrum of this solution shows a product of C_s symmetry, which indicates inequivalent chelate arms but rapid fluxionality via chloride passing through a planar transition state. The ^1H NMR chemical shifts (ranging from +34 to −13 ppm) and the absence of ^{31}P NMR signals indicate paramagnetism; the temperature-dependent ^1H NMR chemical shifts deviate more from the 0−10 ppm region at lower temperatures, consistent with the Curie−Weiss law. Crystals were grown, following trituration with pentane, by treatment of the red oil with Et_2O/pentane.

The crystal structure determination reveals (Figure 2) that the product has not evolved N_2 but contains intact phenyl azide, having oxidized phosphorus to P^V (**3**; eq 4). Consistent with Lewis structure **4** (with Fe binding both N2 and N4), the N4−N3 distance is lengthened by about 0.1 Å over the N2−N3 distance.

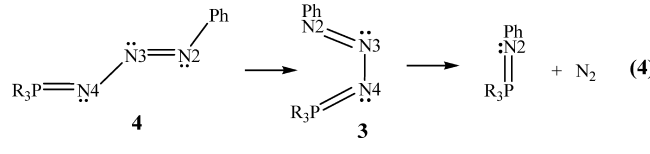

(4)

The N4−P distance is short, consistent with a double bond (1.65 Å). The unit cell contains two crystallographically independent molecules, and this is a rare case where the two are not identical within 3 estimated standard deviations (esd's). Both molecules have iron coordinated to one P,

(15) Ingleson, M. J.; Fullmer, B. C.; Buschhorn, D. T.; Fan, H.; Pink, M.; Huffman, J. C.; Caulton, K. G. *Inorg. Chem.* **2008**, *47*, 407.
(16) Eckert, N. A.; Dinescu, A.; Cundari, T. R.; Holland, P. L. *Inorg. Chem.* **2005**, *44*, 7702.
(17) Iluc, V. M.; Miller, A. J. M.; Hillhouse, G. L. *Chem. Commun.* **2005**, 5091.
(18) See the Supporting Information.

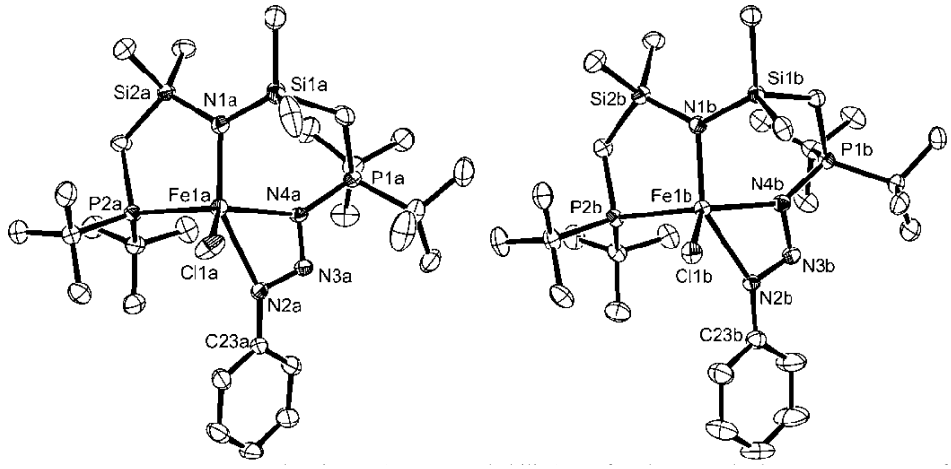

Figure 2. ORTEP drawing (50% probability) of the non-hydrogen atoms of [^{t}Bu$_2$PCH$_2$SiMe$_2$NSiMe$_2$CH$_2$P^{t}Bu$_2$N$_3$Ph]FeCl, showing selected atom labeling of molecules a and b. Unlabeled atoms are carbon. Selected structural parameters (molecules a and b): Fe1−N1, 2.0439(17) and 2.0359(16) Å; Fe1−N2, 2.4422(17) and 2.3283(16) Å; Fe1−N4, 2.1290(17) and 2.2099(16) Å; Fe1−Cl 1, 2.2971(6) and 2.3062(6) Å; Fe1−P2, 2.4860(6) and 2.5015(6) Å; P1−N4, 1.6538(17) and 1.6587(16) Å; N2−N3, 1.271(2) and 1.278(2) Å; N2−C23, 1.422(3) and 1.421(3) Å; N3−N4, 1.360(2) and 1.347(2) Å.

amide N, and Cl and N2 and N4 of the Staudinger adduct, but the Fe−N4 distances differ by 0.08 Å (20 esd's) and the Fe−N2 distances differ by 0.11 Å (57 esd's). Thus, while iron in both molecules is five-coordinate and both have N4 bonded closer to iron than N2, there is a shift toward more asymmetric bonding of the two nitrogens in molecule a. This occurs with no change in the N−N distances of more than 0.01 Å. We interpret this unusual variability of bidentate binding of the PhN_3PR_3 unit to it being fundamentally weak, at least as a bidentate form: when one bond weakens, the other strengthens. Such a compensation is especially effective because the bite angle of the ligand is so small (~56°). The identity of this product contrasts with those from the reaction of PhN_3 with (PNP)M for M = Co and Ni. For Fe^{II}, the reduction of the number of d electrons by 2 (vs Co^I) and 3 (vs Ni^I) opens up orbitals that, in effect, trap an intermediate in phosphinimine formation and show that P−N bond formation does not happen at the FeNPh stage but instead even earlier. Nevertheless, this molecule is robust against N_2 loss: it can be recovered unchanged after 12 h at 90 °C in toluene.

The conversion of a phosphine to a phosphinimine is a known and facile reaction of a free phosphine (eq 4), and it occurs via Staudinger intermediate **3**.[19,20] The lone pair of a coordinated phosphine is, in effect, masked or protected, which is what makes a coordinated phosphine less oxygen-sensitive (the thermodynamic product would be $R_3P{=}O$) than is a free phosphine. Thus, "imination" of a phosphine during the reaction of a metal phosphine complex can be interpreted as diagnostic of phosphine dissociation, especially because the metal is oxidized in forming $L_nM(NR)$, and such higher oxidation states (hard Lewis acids) generally have less affinity for a (soft base) R_3P. A reviewer has suggested that the adduct (PNP)Ni(CO) has more Ni−P antibonding character than (PNP)Ni itself,[15] hence favoring Ni−P dissociation in an adduct (PNP)NiL.

Ru^{II}. a. Oxidation of (PNP)RuCl with PhN_3. Ruthenium offers new insights, particularly because we study the ruthenium analogue of the above iron reagent, (PNP)FeCl. The addition of equimolar PhN_3 to (PNP)RuCl[21] in an arene solvent shows evident gas evolution at 25 °C and even at −78 °C, together with the deposition of a red solid. The precipitated product shows no ^{31}P NMR signal, consistent with being paramagnetic, and the ^{1}H NMR spectrum shows six signals with intensity consistent with two different PNP-containing compounds (the phenyl resonances are too weak and too paramagnetically broadened to be reliably assigned). Only the $SiCH_2$ signals of one species lie outside the normal alkyl ^{1}H NMR region, but the three signals for the second PNP species all lie outside the 0−10 ppm region. The crystal structure of the solid (Figure 3) identifies the reason for its low solubility in arenes: it is the salt [(PNP)Ru(NPh)][(PNP)$RuCl_3$]. The monocation is planar with a linear RuNC imide structure, and the monoanion is a *mer*-octahedral species. The cation has nearly ideal planar geometry, with a short [1.716(3) Å] Ru−N2 bond; the Ru−N distance trans to this is somewhat lengthened at 1.994(2) Å. The Ru−N2−C23 angle to the phenyl ipso carbon is essentially linear [177.5(2)°]. The anion is very near to ideal octahedral geometry, with cis angles from 84.8 to 95.0°; deviations are mainly due to constraints of the PNP chelate. The Ru−N(amide) distance is long, at 2.053(3) Å, because the anion is a 17-valence-electron species even without any amide π donation; a π_{Ru-NSi} bond order of 0.5 pertains. Nevertheless, the Ru−Cl distance trans to the amide N is longer (by 0.05 Å) than the two Ru−Cl distances that are mutually trans. Given this knowledge of the composition of the solid, ^{1}H NMR assignments of the solid product described above become clear: one C_{2v} cation (d^4) and one C_{2v} anion (d^5).

b. Zinc Reduction of [(PNP)Ru(NPh)][(PNP)$RuCl_3$]. Derivatization of the salt was sought to further establish its composition. A solution of [(PNP)Ru(NPh)][(PNP)$RuCl_3$] in THF undergoes a color change from bright red to maroon during 1 h of stirring in contact with excess zinc powder.

(19) Dehnicke, K.; Straehle, J. *Polyhedron* **1989**, *8*, 707.

(20) Lin, F. L.; Hoyt, H. M.; Van Halbeek, H.; Bergman, R. G.; Bertozzi, C. R. *J. Am. Chem. Soc.* **2005**, *127*, 2686.

(21) Watson, L. A.; Ozerov, O. V.; Pink, M.; Caulton, K. G. *J. Am. Chem. Soc.* **2003**, *125*, 8426.

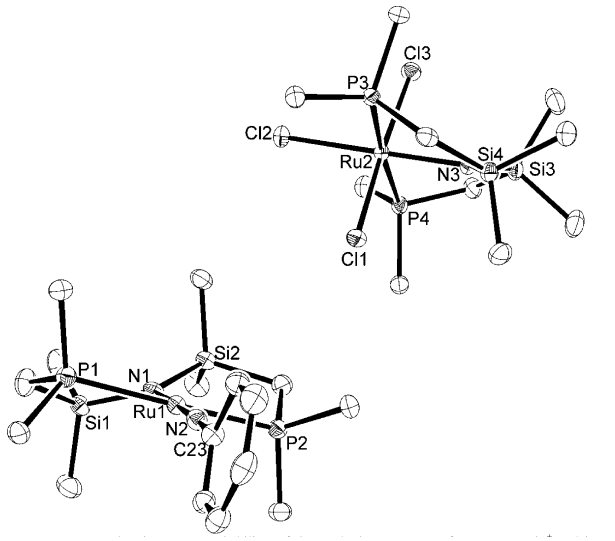

Figure 3. ORTEP drawing (50% probability) of the non-hydrogen atoms of $[PNP]Ru(NPh)^+$ and its counterion $[PNP]RuCl_3^-$, showing selected atom labeling. Unlabeled atoms are carbon, and ^{t}Bu methyls have been omitted. Selected structural parameters: Ru1−N2, 1.716(3) Å; Ru1−N1, 1.994(2) Å; Ru1−P2, 2.4291(9) Å; Ru1−P1, 2.4386(9) Å; C23−N2−Ru1, 177.5(2)°; N2−Ru1−N1, 179.07(12)°; N2−Ru1−P2, 95.27(9)°; N1−Ru1−P2, 84.78(8)°; N2−Ru1−P1, 94.29(9)°; N1−Ru1−P1, 85.66(8)°; P2−Ru1−P1, 170.44(3)°; Ru2−N3, 2.053(3) Å; Ru2−Cl3, 2.3859(8) Å; Ru2−Cl1, 2.3909(8) Å; Ru2−Cl2, 2.4375(8) Å; Ru2−P4, 2.4576(8) Å; Ru2−P3, 2.4646(8) Å; N3−Ru2−Cl3, 87.81(7)°; N3−Ru2−Cl1, 88.87(7)°; Cl3−Ru2−Cl1, 176.67(3)°; N3−Ru2−Cl2, 179.34(8)°; Cl3−Ru2−Cl2, 91.53(3)°; Cl1−Ru2−Cl2, 91.79(3)°; Cl3−Ru2−P4, 94.98(3)°; Cl1−Ru2−P4, 84.87(3)°; Cl2−Ru2−P4, 92.70(3)°; Cl3−Ru2−P3, 85.09(3)°; Cl1−Ru2−P3, 94.76(3)°; Cl2−Ru2−P3, 92.45(3)°; P4−Ru2−P3, 174.85(3)°.

Scheme 1

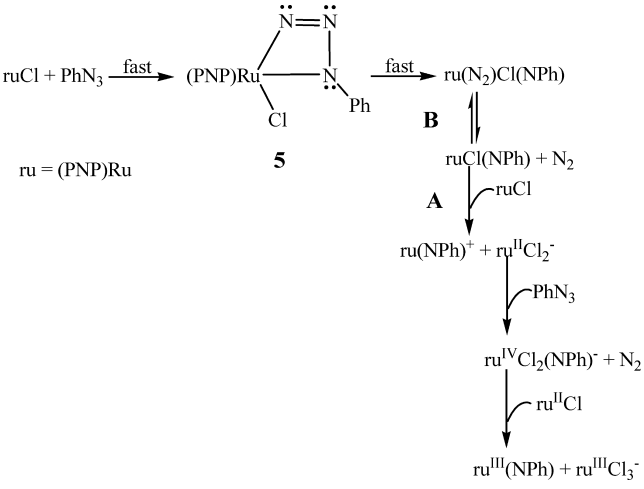

Produced in an equimolar ratio (^{1}H NMR assay) are the known (PNP)RuCl together with another paramagnetic C_{2v}-symmetric species, which we assign as (PNP)Ru(NPh). Zinc thus reduces Ru^{IV} of the cation to Ru^{III} and Ru^{III} of the anion to Ru^{II}. The addition of 4 equiv of PhCN per Ru to a benzene solution of this zinc-reduced mixture converts (PNP)RuCl completely to the known[21] diamagnetic *trans*-(PNP)Ru-$Cl(NCPh)_2$, but free PhCN persists and ^{1}H NMR signals due to (PNP)Ru(NPh) are unchanged, indicating it to be not Lewis acidic toward PhCN.

The X-band electron paramagnetic resonance (EPR) spectrum of (PNP)Ru(NPh) in a toluene solution[18] at 25 °C is a single line at $g = 1.96$, correct for an $S = {}^1/_2$ species, flanked by two of the six lines expected for the 13 and 17% abundant ruthenium isotopes 99 and 101 (both $I = {}^5/_2$), with an A value of about 20 G. There is no resolved hyperfine coupling to any other ligand atoms in the fluid medium. In a frozen glass at −196 °C, the spectrum resolves into three g values, consistent with the planar C_{2v}-symmetric structure. There is incipient ligand hyperfine coupling resolved in two of the three g tensor signals, with all coupling being below 20 G. Coupling to the central g component was modeled by two ^{31}P NMR nuclei, while the coupling in the large g value signal is attributed to one ^{14}N. Given the frontier orbitals calculated (see section d), it is reasonable that coupling to phosphorus is small, and it is reasonable to assign the nitrogen involved in the EPR spectrum as that of the phenylimide ligand because the spin density of the PNP amide nitrogen is very small (see section d). Finally, the g values are significantly shifted from the free electron value, indicating that there is spin density on ruthenium.

c. Overall Balanced Reaction of (PNP)RuCl with PhN_3. The implication of the red crystalline product is that not all redox equivalents are accounted for with only this product. In fact, the supernatant solution that deposits the red crystalline salt is shown by ^{1}H NMR spectroscopy to contain (PNP)Ru(NPh), identical with the product of the zinc reduction. Thus, the overall reaction is shown in eq 5. The total of four redox equivalents in two molecules of PhN_3 thus goes to oxidize three rutheniums by 2, 1, and 1 electrons, respectively, in this reaction.

$$3(PNP)RuCl + 2PhN_3 \rightarrow (PNP)RuNPh^+ + (PNP)RuCl_3^- + (PNP)Ru(NPh) \quad (5)$$

The key point is that this has been redox chemistry, with electron-rich ruthenium being oxidized, in contrast to the iron analogue. As the NPh ligand settles onto the metal, it apparently adopts a linear RuNC geometry, which is enough to weaken the Ru−Cl bond. Chloride is then removed/scavenged by a second initially 14-electron (PNP)RuCl center, which must become more Lewis acidic upon oxidation to Ru^{III} because it again serves as the halide acceptor, generating $(PNP)RuCl_3^-$. The redox balance (eq 6) shows that two phenyl azides consume four electrons.

$$2PhN_3 + 4e^- \rightarrow 2PhN^{2-} + 2N_2 \quad (6)$$

The reason why the reaction does not simply produce molecular (PNP)Ru(NPh)Cl or the salt [(PNP)Ru(NPh)]Cl must lie in the Lewis acidity of (PNP)RuCl, or its Ru^{III} analogue, together with $(PNP)RuCl_3^-$ being inert to PhN_3. The latter is consistent with the idea that PhN_3 is only a redox reagent if it first coordinates to the metal, something that evidently cannot happen with octahedral $(PNP)RuCl_3^-$.

Note also that the reduction of $(PNP)Ru(NPh)^+$ by zinc is also relevant to the production of (PNP)Ru(NPh) in the original reaction because the reductant there is (PNP)RuCl itself, at least until late in the reaction, when this reductant is depleted.

A plausible mechanism for forming the products (Scheme 1) proceeds through an adduct with PhN_3, and then Cl^- lost

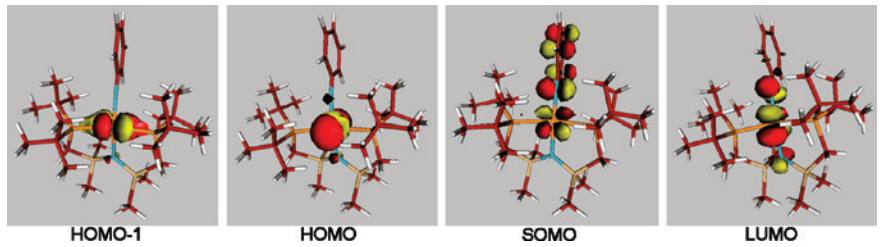

Figure 4. Frontier orbitals of (PNP)Ru(NPh) showing three occupied d orbitals (HOMO-1, HOMO, and SOMO) and spin density on the NPh group, as well as the LUMO.

from that adduct can be scavenged by (PNP)RuCl, to yield N_2, (PNP)Ru(NPh)$^+$, and (PNP)RuCl$_2^-$. The reaction of PhN_3 with this five-coordinate Ru^{II} anion would yield (PNP)RuCl$_2$(NPh)$^-$, which would lose Cl^- to another (PNP)RuCl, together with a chlorine atom transfer, to give the other observed products, N_2, (PNP)Ru(NPh), and (PNP)RuCl$_3^-$. This is attractive in avoiding reactions bimolecular in bulky (PNP)Ru complexes and using the fact that an NPh ligand will tend to expel a ligand as it becomes linear and donates more electrons to ruthenium.

An alternative to reaction A in Scheme 1 is chlorine atom transfer from (PNP)Ru^{IV}Cl(NPh) to (PNP)Ru^{II}Cl, giving observed products (PNP)Ru^{III}(NPh) and (PNP)Ru^{III}Cl$_2$, which will later scavenge Cl^- to give observed (PNP)RuCl$_3^-$. This shows that there are two reactions in competition for available (PNP)RuCl, oxidation by PhN_3 and chlorine (atom or ion) scavenging, which is what leads to the observed 3:2 (PNP)RuCl/PhN_3 stoichiometry in eq 5.

Observations relevant to some of these steps are available from low-temperature monitoring of (PNP)RuCl and PhN_3 reagents combined and held at low temperature prior to low- and variable-temperature ^{1}H and ^{31}P NMR monitoring (see the Experimental Section); the salt (Figure 3) is not detected in these studies in toluene because it is already fully formed at −60 °C but is essentially insoluble in toluene at this temperature. It is important to recognize that new species detected in this soluble portion represent a small fraction of the total yield and are under the special influence of a modest initial excess of the PhN_3 oxidant; in particular, these represent a late stage of the reaction. These spectra show a rapid (^{31}P NMR time scale, hence, one temperature-dependent ^{31}P NMR chemical shift) equilibrium between two diamagnetic molecules, both of which disappear by +20 °C. Diamagnetism indicates that these are both even-electron species and have a coordination number 5 or 6. The ^{1}H NMR spectra recorded concurrently during this study show these time-averaged species to have C_s symmetry (two ^{t}Bu and two SiMe signals). We suggest (Scheme 1, reaction B) that these are (PNP)Ru(N_2)Cl(NPh) and (PNP)RuCl(NPh), where chloride loss has not happened because of depletion of the chloride scavenger and reductant (PNP)RuCl in the late stage of the reaction. Coordination of N_2 is a natural kinetically controlled consequence if the (unobserved) primary product is (PNP)RuCl(N_3Ph); thus, that terminal N of N_2 is bonded to ruthenium prior to N−N bond cleavage, a reaction that may occur by a four-membered ring transition state (**5** in Scheme 1). The structure of (PNPN_3Ph)FeCl shows that a coordinated PhN_3 fragment is capable of forming such a four-membered ring.

Alternative identities for the two diamagnetic species in dynamic equilibrium at low temperature include (PNP)RuCl(N_3Ph), with the phenyl azide bound η^1 through its α- or γ-nitrogen as well as bound η^2 through both of these nitrogens (i.e., species **5**). These remain at low temperature at the end of the reaction, in the presence of excess PhN_3, because there is insufficient (PNP)RuCl to effect either chlorine atom transfer or chloride transfer. However, by 23 °C, these species have decayed, to yield only an array of paramagnetic signals, together with (PNP)Ru(NPh), which was already evident at −60 °C.

d. Density Functional Theory (DFT) Analysis of (PNP)Ru(NPh) Species. DFT (B3LYP) calculations on the redox pair (PNP)Ru(NPh) and (PNP)Ru(NPh)$^+$ were carried out. For the cation, the species characterized in the salt (Figure 3), these show a singlet ground state with the triplet 9.5 kcal/mol higher. In the triplet, the spin density is 1.07e$^-$ on ruthenium but 0.54e$^-$ on N_2 (the amide nitrogen) and 0.32e$^-$ on the phenyl ring, hence highly delocalized, with significant oxidation at the phenylimide ligand. Any singlet-to-triplet conversion thus has metal-to-ligand charge-transfer character (see the Supporting Information). The spin density on the phenyl ring thus naturally accounts for the NMR nonobservance of the phenyl protons, due to rapid relaxation. The highest occupied molecular orbital (HOMO) and HOMO−1 of the singlet cation are the d_{xz} (x along the Ru−P direction) and d_{z^2} orbitals; the lowest unoccupied molecular orbital (LUMO) is the d_π orbital perpendicular to the phenyl ligand plane (i.e., in the Ru−N1−P2 plane) in the antibonding phase with that phenylimide nitrogen and carbon orbitals.[18] Because the triplet is achieved by populating an orbital with Ru−NPh π^* character, the Ru−N distance lengthens by 0.08 Å from singlet to triplet. In the neutral doublet (PNP)Ru(NPh), the same two orbitals are doubly occupied, and the singly occupied molecular orbital (SOMO) closely resembles the LUMO of the singlet cation, as expected for simple one-electron reduction without gross electronic reorganization (Figure 4; see also the Supporting Information). The neutral doublet has 0.31e$^-$ spin density on ruthenium with 0.41e$^-$ on N2 and 0.30e$^-$ on the phenyl ring, hence again considerably delocalized, yet still with a short calculated Ru−N2 distance, 1.81 Å. The SOMO of (PNP)Ru(NPh) and both SOMOs of triplet (PNP)Ru(NPh)$^+$ show negligible participation by phosphorus orbitals, so it is

understandable that the EPR spectra show little or no coupling to those nuclei.

The most distinctive structural difference between the singlet and triplet $(PNP)Ru(NPh)^+$ is the Ru−N2 distance, 1.74 Å for the singlet and 1.82 Å for the triplet. However, because we observe no ^{31}P NMR signal for the species $(PNP)Ru(NPh)^+$ in its salt with the paramagnetic anion $(PNP)RuCl_3^-$, it is difficult to escape the conclusion that $(PNP)Ru(NPh)^+$ is indeed paramagnetic, hence a triplet, unless the NMR features of the cation are influenced by intimate ion pairing with the truly paramagnetic anion. What favors the singlet attribution for $(PNP)Ru(NPh)^+$ is that the calculated singlet Ru−NPh distance (1.74 Å) is in better agreement with the observed value (1.72 Å) than is the triplet. One reviewer disagrees: "...a conclusion about the cation's spin state cannot yet be reached."

Discussion

Perhaps the most important conclusion from the composition and structure of the Fe^{II} product reported here is to show that the formation of the P═N bond does not necessarily require that an electrophilic NPh ligand be present, as is evident from the (metal-free) Staudinger reaction. The intact azide is sufficiently electrophilic to perform two-electron oxidation of P^{III}. Why does this iron complex not rapidly evolve N_2? It is clear from eq 7 that N_2 elimination requires an s-syn conformation around the single N3−N4 bond, while the observed bidentate binding of the P−N4−N3−N2 group imposes an s-anti configuration.

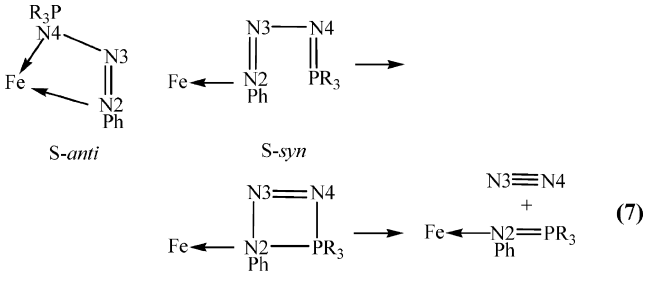

(7)

6

Bidentate binding interferes with the cyclization to form **6** because that cyclization requires rupture of the Fe−N4 bond. This raises the barrier for N_2 elimination, and so the product $[PNP(N_3Ph)]FeCl$ is trapped. The final point is that the decrease of the d electron count to 6, from monovalent Co and Ni, allows the $PNPN_3Ph^-$ ligand to be tetradentate and thus is the origin of the features unique to iron.

The results reported here show a variety of outcomes for $(PNP)MX_n$ complexes in contact with the oxidizing environment of phenyl azide. The results with 3d metals show that attack on the PNP ligand phosphorus is favored over attack at the methyl C−H bonds or at electron-rich amide N (forming **7**); a reducing metal is required, however, because (PNP)NiCl is inert to PhN_3. The reaction of $IrCl_2L_3^+$ (L = PR_3) with $PhCH_2N_3$ gives an adduct of intact azide, which then loses N_2, to give[22] $Cl_2L_3Ir^{III}[N(H)═CHPh]^+$ rather than isomeric $Cl_2L_3Ir(═NCH_2Ph)^+$. This is a case where oxidation of benzylic carbon is favored over oxidation of trivalent iridium. In addition, the $Cl_2L_3Ir^V(═NCH_2Ph)^+$ alternative would have a bent imide ligand, with a nitrogen lone pair that is probably a reactive site.

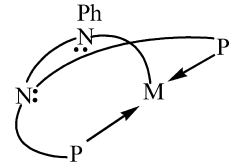

7

Work with electron-rich (PNP)RuCl shows that the metal is the preferred reductant, even if the thermodynamic product might have been [PNP(═NPh)]RuCl, so the reaction may be under kinetic control. The high rates to all observed products indicate that electron transfer is facile when it is thermodynamically favored.

$(PNP)Ru^{IV}(NPh)^+$ is a 16/18-electron, planar d^4 species (counting a triple Ru−NPh bond), which is the formal product of transferring $C_6H_5^+$ to the nitride of known[23] (PNP)RuN. The Ru−N distance in this nitride is 1.627(2) Å, or 0.09 Å shorter (vs Figure 3) because the nitrogen was made more nucleophilic but still triply bonded to ruthenium. One point of interest is that, while d^4 (PNP)RuN is diamagnetic,[23] the addition of a $C_6H_5^+$ electrophile to the nitride nitrogen yields a triplet ground state. Why is this? One answer might be that the addition of this electrophile to nitride nitrogen weakens the ligand field, hence leading to smaller orbital energy spacings and high spin behavior.

The reaction of phenyl azide with (PNP)RuCl is exceptionally complex because four-coordinate Ru^{II} here is not only a reducing agent but also a Lewis acid (hence scavenging ionic chloride) and a primary product $(PNP)RuCl(N_3Ph)$ has M−P bonds that are more kinetically inert than those of (PNP)FeCl. The observed chemistry of PhN_3 with (PNP)FeCl shows what happens when metal-based redox chemistry (including N_2 loss) is not favorable, so another reaction channel (i.e., mechanism) intervenes. That reaction channel is influenced by empty orbitals in $S = 1$ (PNP)RuCl, in contrast to all orbitals at least half-filled in $S = 2$ (PNP)FeCl. The other reaction channel uses the additional available iron orbital (even if spin pairing is required) and thus can stop without oxidation of iron to Fe^{IV}, whereas those preferences are reversed for (PNP)RuCl. In the case of monovalent nickel, why is the redox reaction so fast even at −60 °C, with no intermediate detectable even there, and likewise no (PNP)Ni(NPh) detectable? We suggest that, finally for the d^9 configuration among the 3d configurations studied here, a linear NiNPh moiety in (PNP)Ni(NPh) displaces one phosphine arm to avoid a 19-electron configuration and favor a 17-electron count (thus using all nine valence orbitals, even

(22) Albertin, G.; Antoniutti, S.; Baldan, D.; Castro, J.; Garcia-Fontan, S. *Inorg. Chem.* **2008**, *47*, 742.
(23) Walstrom, A.; Pink, M.; Yang, X.; Tomaszewski, J.; Baik, M.-H.; Caulton, K. G. *J. Am. Chem. Soc.* **2005**, *127*, 5330.

if one is only singly occupied). The pendant phosphine is then sufficiently nucleophilic and reducing to attack the phenylimide nitrogen, leading to the observed product. The complete lack of spectroscopic change for (PNP)NiCl in the presence of PhN_3 shows that any adduct between these two has a very small binding constant for an η^1 adduct (PNP)NiCl(N_3Ph) and certainly lacks enough valence orbitals to bind PhN_3 in an η^2 fashion,[17] which we believe is central to breaking the N−N bond after two-electron transfer has taken place. η^1 binding is not conducive to breaking of the $N_\alpha-N_\beta$ bond, even after two-electron transfer (**8**, which shows that it is the $N_\gamma-N_\beta$ bond that is weakened), but certain resonance forms of η^2-RN_3 are conducive to scission of this bond (**10** and **11** vs **9**). The fact that phosphorus is not oxidized in the ruthenium case probably results from the Ru−P bonds being kinetically inert, so there is no nucleophilic phosphorus to attack electrophilic nitrogen. η^1 binding at N_α is sterically unfavorable.

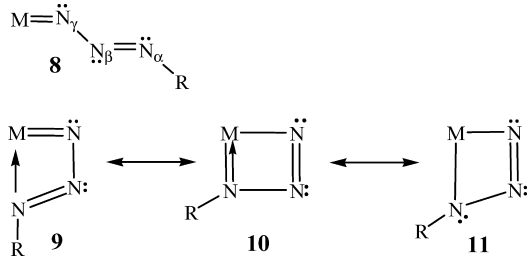

Finally, attack on the ancillary ligand observed here for the 3d metals must be seen as a general example[22,24] of "ligand degradation", which needs to be taken into account in seeking application for a given ligand type. Here, the nucleophilic character of the PNP ligand is evident under electrophilic conditions, which redirects future attention to applications of PNP under reducing conditions. On the other hand, the synthesis of (PNP)Ru(NPh) here suggests that isoelectronic (PNP)RuO might be a realistic synthetic target and that (PNP)Ru(O)Cl might be a useful oxidant.

Experimental Section

General Considerations. Preparations from literature sources were used to synthesize starting materials RuN(SiMe$_2$-CH$_2$P^{t}Bu$_2$)$_2$Cl,[21] (PNP)Ni,[15] and (PNP)FeCl,[15] and standard Schlenk or glovebox techniques in an inert (argon) atmosphere were used for air-sensitive manipulations. All solvents, including deuterated NMR solvents, were dried over and distilled from Na/benzophenone and stored in anaerobic conditions. All other reagents were degassed and/or used as received from commercial vendors. ^{1}H and ^{31}P{^{1}H} NMR spectra were recorded on a Varian Unity I400 (400 MHz ^{1}H and 162 MHz ^{31}P{^{1}H}) instrument, with chemical shifts reported in ppm, referenced to protio impurities in each stated solvent, and ^{31}P{^{1}H} spectra were externally referenced to 85% H_3PO_4 (0 ppm). FT-IR spectra were recorded on a Nicolet 510P spectrophotometer. Mass spectra (ESI-MS) were acquired on a PE-Sciex API III triple-quadrupole spectrometer and simulated with IsoPro 3.0 isotopic distribution software.

[(^{t}Bu$_2$PCH$_2$SiMe$_2$)N(SiMe$_2$CH$_2$^{t}Bu$_2$*P*═NPh)]Ni. To a solution of 15 mg (0.030 mmol) of (PNP)Ni in 0.5 mL of C_6D_6 was added in a J-Young NMR tube at 25 °C 3 μL (0.027mmol) of PhN_3. The solution went from pale yellow to yellow brown, and gas bubbles were observed. The solution was stripped to dryness in a vacuum; the solid was then dissolved in minimal pentane and cooled to −40 °C for 24 h. Yellow crystals formed, suitable for X-ray diffraction study. The solution was decanted, and the crystals were washed with cold pentane and then dried by a vacuum. ^{1}H NMR (25 °C, C_6D_6): δ 16.8 (vbs, 2H, CH_2), 8.8 (vbs, 12H, SiMe), 4.6 (vbs, 36H, ^{t}Bu), −24.6 (vbs, CH_2). ^{1}H NMR (−30 °C, C_7D_8): δ 19 (vbs, 2H, CH_2), 10.6 (vbs, 12H, SiMe), 4.9 (vbs, 18H, ^{t}Bu), 3.9 (vbs, 18H, ^{t}Bu), −24.8 (vbs, 2H, CH_2). At this temperature, it is clear that the ^{t}Bu peaks resolve into two separate signals, which implies accidental degeneracy at 25 °C. ESI MS (THF): *m*/*z* 597 and 599 ((PNPN-Ph)NiH$^+$) for ^{58}Ni and ^{60}Ni.

Reaction of (PNP)FeCl with Phenyl Azide (PhN_3). To a Teflon-sealed reaction flask containing 12.5 mg of (PNP)FeCl (0.0231 mmol) dissolved in toluene-d_8 and chilled in a dry ice/acetone bath was added an equimolar amount of phenyl azide. Upon warming to room temperature with stirring, a sharp color change from the characteristic light brown of the starting material to deep maroon occurred. The resulting solution was analyzed by NMR [see below; conversion of (PNP)FeCl was complete, and only one product was formed in >90% yield], and then the volatiles were stripped in a vacuum. The resulting oil was triturated with pentane several times, followed by a 10% ether/pentane mixture. A small crop of deep-red orthorhombic crystals was isolated and analyzed by X-ray diffraction. A portion of the mother liquor was analyzed by FT-IR, with the only peak of interest found above 1000 cm^{-1} being ν 1591 cm^{-1}. Upon attempted thermolysis in a J-Young NMR tube for 12 h with a 90 °C oil bath, the sample experienced no color or ^{1}H NMR change. ^{1}H NMR (400 MHz, C_7D_8): δ 34 (br s, 18H, P^t*Bu*$_2$), 31 (br s, 2H, Si−C*H*$_2$−P), 23 (br s, 6H, Si−*Me*$_2$), 15 (br s, 6H, Si−*Me*$_2$), 13 (br s, 2H, Si−C*H*$_2$−P), 9.7 (br s, N$_3$−*Ph*$_{aryl}$), 5.7 (br s, N$_3$−*Ph*$_{aryl}$), −2.3 (br s, N$_3$−*Ph*$_{aryl}$), −13 (br s, 18H, P−^{t}*Bu*$_2$). The assignment of signals to silyl Me and ^{t}Bu groups was done by relative integration values. The assignment of the intensity 2 methylene protons and phenyl protons was more difficult and therefore more tentative; the most separated, 31 and 13 ppm, are assigned to CH_2 protons, based on their proximity to the iron center.

Reaction of (PNP)RuCl with Phenyl Azide (PhN_3). Room Temperature Experiment. To a J-Young NMR tube containing 15.3 mg (0.0257 mmol) of (PNP)RuCl in C_6D_6 was added 3.1 mg (approximately 1 mol equiv) of neat PhN_3. Upon separation of the precipitated red crystalline product, comprised of pure [(PNP)RuNPh]$^+$[(PNP)RuCl$_3$]$^-$, and preparation of a saturated THF-d_8 solution, the following were obtained. ^{1}H NMR (400 MHz, THF-d_8): δ 19.58 (4H, CH_2 of (PNP)RuCl$_3^-$), 10.26 (12H, $SiMe_2$ of (PNP)RuCl$_3^-$), 1.81 (36H, P^{t}Bu$_2$ of (PNP)RuNPh$^+$), 0.30 (12H, $SiMe_2$ of (PNP)RuNPh$^+$), −0.92 (4H, CH_2 of (PNP)RuNPh$^+$), −2.63 (36H, P^{t}Bu$_2$ of (PNP)RuCl$_3^-$). Assignments of any two signals of equal intensity were done assuming the broader, more shifted signals are due to the anion. ^{31}P{^{1}H} NMR (162 MHz, THF-d_8): no signals in the δ −500 to +500 range. FT-IR (solid on a KBr plate): ν(Ru═N) 1261 cm^{-1}. ESI-MS (THF, positive ion detection): *m*/*z* 641.2 ((PNP)RuNPh$^+$). THF is also an acceptable solvent for this reaction, but if the reaction is carried out in pentane

(24) Gregory, E. A.; Lachicotte, R. J.; Holland, P. L. *Organometallics* **2005**, *24*, 1803.

or diethyl ether, [(PNP)Ru(NPh)][(PNP)$RuCl_3$] is not produced. Attempts to precipitate salts containing only (PNP)Ru(NPh)$^+$ failed using $NaBPh_4$ or $TlPF_6$.

Variable-Temperature Experiment. To a J-Young NMR tube containing 20.3 mg (0.0342 mmol) of (PNP)RuCl in C_7D_8 at −78 °C (dry ice/acetone bath) was added by a cannula a solution containing 4.0 mg of PhN_3 in C_7D_8. The tube was immediately frozen in liquid N_2 and kept frozen until it was inserted into a precooled NMR probe. When the sample was placed into the instrument, the sample was briefly shaken vigorously to ensure homogeneity. First, spectra were obtained at −60 °C and then repeated in 10 °C increments, waiting 15 min for thermal equilibration at each new temperature.

Already at −60 °C, all (PNP)RuCl had been consumed, and the solution color has changed to dark purple, small red crystals began to form, and the solution phase showed a $^{31}P\{^1H\}$ NMR singlet (0.3 ppm broad), together with two ^{t}Bu ^{1}H NMR and two SiMe signals consistent with diastereotopically inequivalent P^{t}Bu$_2$ and $SiMe_2$ groups but mirror symmetry relating the two arms of the PNP ligand. As the temperature is increased in 10 °C increments, no new compounds form up to −20 °C. However, the ^{31}P NMR chemical shift moves dramatically as the temperature rises, from δ +37 at −60 °C to δ +48 at −20 °C. At +20 °C, this signal is at δ +77 but of diminished integrated intensity. The two ^{t}Bu signals also clearly decline in intensity beginning at about −20 °C and then are very weak by +20 °C. These observations are consistent with temperature-dependent equilibrium between two diamagnetic species. An adduct (PNP)Ru(PhN_3)Cl will make the two groups on a P^{t}Bu$_2$ or $SiMe_2$ inequivalent, and this adduct would have decreasing mole fraction as the temperature rises because of the unfavorable entropy change to form the adduct. If the observed ^{31}P NMR signal is a mole-fraction-weighted average of the two equilibrating complexes, this explains the observations. Other features bear mention: even at −60 °C, a weaker $^{31}P\{^1H\}$ NMR signal of unidentified origin is observed, at δ +55, but this does not change in chemical shift or grow in intensity with increased temperature, suggesting it to be some product formed only on initial local heating when the reagents were combined at −78 °C; this signal is still present (sharp at 56 ppm) in the NMR spectrum at +20 °C, but it decays completely and irreversibly after 3 h at 25 °C. A ^{t}Bu apparent virtual triplet in the ^{1}H NMR (∼1.48 ppm) is observed at every temperature and with constant intensity, which we therefore assign to the species with the δ +55 ^{31}P chemical shift; it finally decays after 3 h at 25 °C. In addition, the ^{1}H NMR spectra from −10 to +20 °C show a broad peak at δ +5.4−5.6, due to (PNP)Ru(NPh). Red crystals persist at 22 °C at the end of this study.

Other Attempted Oxidations. For comparison, equimolar (PNP)RuCl and PhN═NPh in THF-d_8 show unreacted starting materials (NMR assay) even after heating at 65 °C for 24 h.

For some combination of electronic and steric effects, adamantyl azide does not react with PNPRuCl: the reagents (equimolar, in benzene) are recovered unchanged after 20 h at 65 °C.

Zinc Reduction of [(PNP)Ru(NPh)]$^+$[(PNP)$RuCl_3$]$^-$. To a J-Young tube containing 50 mg of [(PNP)Ru(NPh)][(PNP)$RuCl_3$] in THF-d_8 was added a 10-fold excess of activated (by HCl) zinc powder. This mixture was allowed to rotate overnight, and after 15 h, the ^{1}H NMR spectrum showed complete reduction to a 1:1 mixture of (PNP)Ru(NPh) and (PNP)RuCl, with the latter identified by comparison to an authentic sample. NMR yield: >90% (no other products detected). ^{1}H NMR (400 MHz, THF-d_8): δ 5.36 (36H, P^t*Bu* of (PNP)Ru(NPh)), 0.42 (12H, Si*Me*$_2$ of (PNP)Ru(NPh)), −5.01 (4H, C*H*$_2$ of (PNP)Ru(NPh)). $^{31}P\{^1H\}$ NMR (162 MHz, THF-d_8): no signal in the δ −500 to +500 range.

Reaction of a 1:1 (PNP)Ru(NPh)/(PNP)RuCl Mixture with PhCN. To a J-Young tube containing 10 mg of a 1:1 (PNP)Ru(NPh)/(PNP)RuCl mixture was added 7.5 μL (approximately 4 mol equiv per ruthenium) of PhCN. The red color of the sample intensified immediately, and an immediate ^{1}H NMR spectrum showed complete conversion of (PNP)RuCl to the known molecule (PNP)RuCl(PhCN)$_2$ and showed no reactivity of (PNP)Ru(NPh) toward PhCN (free PhCN was observed and (PNP)Ru(NPh) remained unchanged). The solvent was then stripped and the resulting residue extracted with pentane, effectively separating the two compounds because of the extremely poor solubility of (PNP)RuCl(PhCN)$_2$ in pentane. ESI-MS of the neutral (PNP)Ru(NPh), separated from the pentane-insoluble (PNP)RuCl(PhCN)$_2$, was obtained and showed *m*/*z* 641.25 ((PNP)RuNPh$^+$).

Acknowledgment. This work was supported by the NSF (Grant CHE-0544829). We thank Prof. Daniel Mindiola for useful discussions and suggestions.

Supporting Information Available: CIF files for three molecules, plots of NMR spectra, a least-squares fit of (PNP═NPh)Ni versus (PNP═]NPh)Co, EPR spectra of (PNP)Ru(NPh), and DFT results for (PNP)Ru(NPh)$^{0,+}$. This material is available free of charge via the Internet at http://pubs.acs.org.

IC801035Z